C^k-Generalized FEM with enhanced consistency: application to the static elastic rod deformation problem

Diego Amadeu F. Torres

Dept. of Mechanical Engineering, Federal University of Technology of Paraná
Avenida João Miguel Caram 3131 Jd. Morumbi, 86036-370, Paraná, Brazil
diego.amadeu@gmail.com

Abstract. The C^k-Generalized Finite Element Method (C^k-GFEM) in its original version considers Partition of Unity (PoU) functions defined as Shepard ones, which delivers zeroth order consistency in the absence of uniform polynomial extrinsic enrichment of degree one, at least. Such a feature can make C^k-GFEM unfavorable against the conventional G/XFEM when comparing the degrees-of-freedom (dof) amount for a certain error level. This inconvenience can be overcome through intrinsic enrichment using the Moving Least Squares Method (MLSM), which allows the construction of PoU functions with enhanced polynomial reproducibility despite the cost of demanding the widening of the associated supports. In this context, the present work summarizes some results for the static rod deformation problem, for the linear elasticity, considering different classes of PoU functions and different extrinsic enrichment functions, through an approach that adjusts the k-order of continuity and the p-polynomial degree of the ansatz independently, for some kinds of loads distributions which leads to different classes of solutions. It can be seen that such an improved version enables less dependence concerning the enriched zone size, as already shown when using the original C^k-GFEM, while retaining the smaller cost in terms of dof as the C^0 counterpart.

Keywords: smooth approximations, enhanced consistency, C^k-GFEM, k-p-refinements, enrichment

1 Introduction

The C^k-GFEM [1] was proposed as an alternative for generating approximations with high smoothness, similar to some obtained by mesh-free methods while maintaining the implementation characteristics of G/XFEM. The main difference with the original version of the method is the way the PoU functions are created. Considering polygonal partitioning for a two-dimensional domain, conveniently smooth edge functions are defined from all boundary segments of a nodal cloud, through which the corresponding nodal weighting functions are constructed.

The latter, therefore, inherits the minimum smoothness exhibited by the cloud edge functions. The PoU functions are created in the sequence using the *Shepard* equation, which is nothing more than an MLS approximation of degree zero. This point, mostly, is responsible for a highly relevant aspect that has made the C^k-GFEM not as attractive as conventional GFEM, whose PoU functions are finite element shape functions, ensuring the linear consistency of the approximation.

Although the C^k-GFEM can locally improve the approximation in the neighborhood of stress concentrations represented through extrinsic enrichment [2, 3], and still be less sensitive to the size of the enriched zone, it can demand more degrees of freedom for a given level of a global error[1] compared to its counterpart [4–7]. It can also be argued that the C^k-GFEM demands a higher numerical integration cost. However, it must be noted that this integration cost may be associated not only with the PoU functions, but also with the enrichment functions. Additionally, in previous works, highly exhaustive integration quadratures have been preferred to guarantee negligible integration errors[2].

A rational smooth PoU function, as the Shepard one, will have a more oscillating derivative the smaller its support is, whose extreme values are higher the higher its regularity is. In this context, a motivation to move back towards one-dimensional problems is due to the performance comparison provided by [8] in which different strategies designed to allow higher-order approximations, both in terms of smoothness and polynomial reproducibility,

[1] As the strain energy or energy norm, for example.

[2] Probably, for everyday applications, it would be possible to reduce this effort. Some findings in [5] point towards this direction. A more detailed investigation into this needs to be carried out.

were exploited in situations with high stress concentrations. Special enrichment functions were not used in the case of extrinsically enriched approaches, and the discussion was concerned with the discretization parameters p and h, although making the different smoothness evident. However, the most important issue to highlight is that among the strategies analyzed, C^k-GFEM was the only with the maximum smoothness, $k = \infty$, which makes its approximation subspace much more restricted than the other approaches.

It should be noted that the C^k-GFEM can provide approximations with different orders of smoothness simply by changing the edge functions used in generating the weighting functions [4]. This smoothness adjustment process can be done completely independent of the polynomial degree that is intended to be applied through extrinsic enrichment, i.e., enabling completely decoupled p and k refinements.

Therefore, the present study seeks to overcome the deficiencies of the method and highlight its particularities. The results will be discussed to emphasize the accuracy and convergence capabilities, in terms of strain energy, and stability of the approximations, focusing mainly on the effects of enriched zone sizes when applying special enrichment functions.

2 Model problem

A first application of the proposed strategy was presented by [9], in which static rod deformation problems were solved considering only polynomial functions as extrinsic enrichment. Some advantages could be achieved in terms of error levels and even improving convergence rates but consuming the same number of degrees of freedom that the conventional C^0-GFEM for a given polynomial degree approximation ansatz. However, it is still necessary to assess its performance when using different extrinsic enrichment functions to represent stress concentrations.

The equilibrium equation in strong-form for the model problem considered herein is

$$\frac{d}{dx}\left(A(x)E(x)\frac{d}{dx}u(x)\right) + b(x) = 0 \ , \text{ in } \Omega \ , \tag{1}$$

where $b(x) \in \mathcal{L}(\Omega, \mathbb{R}^1)$ is a distributed load, in [N/m], supposed in the space of *Lebesgue* square-integrable functions on the domain Ω, a open subset in $\mathbb{R}^1$ with boundary $\partial\Omega$. Thus, the solution $u(x) \in \mathcal{H}^2(\Omega, \mathbb{R}^1)$, the *Hilbert* space of functions which with their derivatives up to second order are square-integrable, is the displacement field, which has [m] unit. Herein, the stress concentrations will be caused by some special $b(x)$ load distribution functions.

The variables involved are defined as usual, following classical texts on the topic [10]. For the problems solved herein, it is supposed constant cross-sectional area A, [m^2], and Young's module E, [N/m^2], for simplicity, and it is assumed homogeneous *Dirichlet* and/or *Neumann* boundary conditions without loss of generality. The discretized weakened equilibrium problem is formulated in its irreducible version, using the linear constitutive relation $\sigma(x) = E\varepsilon(x)$, and the infinitesimal strain-displacement relationship $\varepsilon(x) = \frac{d}{dx}u(x)$, being σ and ε the stress and strain, respectively, measured in [N/m^2] and [m/m]. In this context, the strain energy, [J], defined as

$$\mathcal{U}\big(u(x)\big) = \frac{1}{2}\mathcal{B}\big(u(x), u(x)\big) \equiv \frac{1}{2}\int_\Omega EA\left[\frac{d}{dx}\big(u(x)\big)\right]^2 dx \ , \tag{2}$$

with $\mathcal{B}(\bullet, \bullet)$ being the bi-linear form in the correspondent variational version, may be a metric for qualifying the results.

3 Methodology

The procedure for constructing the *weighting* functions can be briefly described as: for each inner node in the discretization it is necessary to build two boundary functions[3], associated with the left and the right boundaries of the corresponding *cloud*. For the boundary nodes, only the internal boundary function is needed. Such boundary functions need to have as many zero derivatives at their corresponding cloud ends to ensure the smoothness intended. For the conventional C^k-GFEM a cloud involves the two elements around its node whereas for the approach with enhanced consistency widened clouds are demanded. In this work, a widened nodal cloud considers the two elements to either the left or right of a given node[4], to guarantee the realization of the MLS with degree one.

For the smooth approximations herein, a uniform k-refinement[5] is obtained by considering boundary functions with different continuities, such that $k = 1, 2, 3$ can be achieved using polynomial boundary functions with

[3]The boundary functions herein are analogous to the cloud edge functions in [1, 7].

[4]For internal nodes adjacent to those on the boundary, a ghost element outside the domain is created.

[5]Different orders of smoothness may be produced simply by choosing different boundary functions along the domain.

polynomial degree $p = 2, 3, 4$, respectively [4]. On the other hand, the maximum continuity, $k = \infty$, is obtained applying exponential boundary functions [1]. Consequently, the *weighting* functions inherit the continuity from the boundary functions. Thus, the PoU functions are MLS functions, having degree zero (Shepard equation) for the C^k-GFEM, and degree one for its version with enhanced consistency/reproducibility. Hereafter, this enhanced version will be referred to as MLS-PoU-based approach.

Different approximation challenges were caused by conveniently choosing force distributions of interesting classes. Firstly, it was considered a situation with a sixth-degree polynomial solution, caused by an excitation $b_1(x)$ acting on a domain $\Omega = [0; 3.0\text{ m}]$, with both ends fixed. In the sequence, it was applied a load distribution $b_2(x)$ which leads to a smooth solution with high derivatives around the position x_0, whose intensity is governed by a parameter α, according to [11]. In this case, a domain $\Omega = [0; 1.0\text{ m}]$, with both ends fixed, was considered. Finally, a load distribution $b_3(x)$ leading to a solution whose derivative shows a singularity at the left end, following [12], was considered. For this, $\Omega = [0; 1.0\text{ m}]$, with the left and right ends fixed and free, respectively. The expressions for such loads are

$$\begin{aligned} b_1(x) &= (7/2)x^4 - 10x^3 + 2x^2 + 5x + 1\ , \\ b_2(x) &= 2\alpha\left[\frac{1}{1+\alpha^2(x-x_0)^2} + \frac{\alpha^2(x-x_0)(1-x)}{\left[1+\alpha^2(x-x_0)^2\right]^2}\right]\ , \text{ and} \\ b_3(x) &= \lambda(\lambda-1)x^{\lambda-2}\ , \end{aligned} \tag{3}$$

and the associated strain energies, measured in [J], for $EA = 1.0$ [N], considering $x_0 = 4/9$ [m] and $\alpha = 50$ as well as $\lambda = 0.65$ for the last two cases, respectively, are the following

$$\mathcal{U}(u_1) = 6.156\,818\,181\,818\,181\ ,\ \mathcal{U}(u_2) = 12.134\,685\,458\,546\,76\ ,\ \text{and}\ \mathcal{U}(u_3) = 0.265\,416\,666\,666\,667 \tag{4}$$

where the explicit dependence on x of the displacement fields was omitted to simplify the notation.

A set of four uniform nested meshes, with $5, 10, 20$, and 40 elements, denoted as M5, M10, M20 and M40, respectively, was chosen to guarantee the inclusion property[6] in case of essentially polynomial sub-spaces.

Only uniform polynomial extrinsic enrichment was applied for the case with a polynomial solution. Differently, special extrinsic enrichments were locally applied, besides the polynomial one, for problems whose solutions exhibit high derivatives. The exact solutions themselves, $u_2(x)$ and $u_3(x)$, respectively, were used as enrichments, being applied to a set of nodes via different schemes, aiming to observe the influence of the enriched zone size, similarly as previously done for C^k-GFEM [2, 3, 7].

For the case with $b_2(x)$, the special enrichment was initially applied to the nodes just around the position x_0, the red nodes in Fig. 1. The collection of nodes was progressively increased, including those right next to the previously enriched ones, i.e., the blue nodes at a second step, the green ones at a third step, and so on. On the other hand, for the case with $b_3(x)$, the special enrichment was also applied to a progressively growing collection of nodes. For each mesh, the final dimension of the enriched zone was defined so that it allows, later, to obtain h-convergence behavior under the condition of the well-known geometric pattern[7] of enrichment, see Fig. 2.

Figure 1. Localized enrichment scheme, with a progressively increasing enriched zone, for the mesh M20.

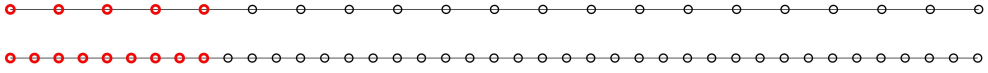

Figure 2. Localized enrichment scheme, with a fixed size enriched zone, for the meshes M20 and M40.

Except for the C^0-GFEM when only polynomial enrichments are used, the needed amount of integration points can not be estimated since the basis functions are not essentially polynomial. Thus, the numerical integration quality for both elemental stiffness matrices and load vectors, $\mathbf{K}_e$ and $\mathbf{F}_e$, respectively, was ensured by using

[6] If the associated functions subspace of a given mesh is contained in the associated functions subspace of the next one them the error decreases from mesh to mesh monotonically as $h \to 0$ [10].

[7] The so-called geometric pattern of enrichment requires that the size of the enriched zone remains fixed as the mesh is refined.

progressively growing Gauss-Legendre quadrature rules, in each element, until a relative deviation reached a pre-established tolerance. For this, the following metrics were used

$$\|\mathbf{K}_e\| = \sqrt{\sum_{i=1}^{\text{dof}_e}\sum_{j=1}^{\text{dof}_e} k_{ij}^2} \quad \text{and} \quad \|\mathbf{F}_e\| = \sqrt{\sum_{i=1}^{\text{dof}_e} f_i^2}\,, \tag{5}$$

where dof_e is the number of dof for a given element. A relative deviation between the entities obtained with the $k-1$ and k-th quadratures was computed by

$$\text{rel. dev.} = \frac{\left(\|\bullet\|^k - \|\bullet\|^{k-1}\right)}{\|\bullet\|^{k-1}}\,. \tag{6}$$

The tolerance was specified as 10^{-11} for both $\mathbf{K}_e$ and $\mathbf{F}_e$, for all methodologies, for the two first load distributions. Differently, for the problem with singular stress field, 10^{-2} was considered for $\mathbf{F}_e$, for all approaches, whereas for $\mathbf{K}_e$, it was necessary to adjust the tolerance to 10^{-9}, for the C^0- and C^k-GFEMs, and 5×10^{-9} for the MLS-PoU-based GFEM. The MLS-PoU-based approximations can demand a less restrictive tolerance because their computation involves rather more operations besides the solution of a point-wise system of equations, which can cause oscillations[8] of the norms in eq. (5).

All the systems of linear algebraic equations were solved via the well established Babuška iterative procedure [13], using a perturbation $\epsilon = 10^{-10}$ and $tol = 10^{-12}$, even if the methodology does not lead to a singular constrained stiffness matrix.

In the sequence, the discussion is carried out to highlight the benefits of different smoothness orders on the way the enrichments are performed, considering plots of relative error versus the number of dof. Such a relative error for an approximation $\tilde{u}(x)$ is defined as

$$\text{rel. error}\ (\%) = \frac{\left|\mathcal{U}(u) - \mathcal{U}(\tilde{u})\right|}{\mathcal{U}(u)}\cdot 100\%\,. \tag{7}$$

Finally, the stability of the approximations is measured by the condition number associated with the constrained stiffness matrices for the problem involving singularity. To enable such a comparison between all the approaches, it was considered a condition number computed as

$$\text{cond. number} = \frac{\lambda_M}{\lambda_m} \tag{8}$$

where λ_M is the larger eigenvalue and λ_m is the smaller nonzero eigenvalue, since the C^0-GFEM and the MLS-PoU-based methodology suffer from linear dependence once polynomial enrichment is extrinsic applied throughout the domain.

4 Results and discussion

Next, the comments are grouped for each of the chosen loads. It should be remarked that as the polynomial degree spanned by the basis functions depends both on the degree of the PoU itself and on the extrinsically polynomial enrichment applied, it has been customary in previous works [2, 3, 5–7] to consider b as the resulting degree of an approximation. Thus, for the C^0-GFEM as well as for the MLS-PoU-based approach, $b = p+1$, with p being the degree of the extrinsic enrichment. Then, for a given degree b, the C^k-GFEM requires more extrinsic polynomial enrichment, generating more dof, consequently.

4.1 Sixth-degree polynomial solution

Figures 3(a) and (b) show the h-convergence for approximations with uniform degree $b = 1$ and $b = 2$, respectively. The error level for all MLS-PoU-based solutions is lower than that for C^0-GFEM. Notably, the order of smoothness affects both the error level and its rate of decrease between two successive meshes. Such an effect is more pronounced when $b = 1$, for the MLS-PoU-based solutions, and when $b = 2$ for the C^k-GFEM.

Yet, when $b = 1$, for the coarsest mesh, the error level for all C^k-GFEM solutions is slightly lower than the C^0-counterpart. When $b = 2$, $C^{2,3}$-GFEM solutions exhibit errors quite similar to those from the MLS-PoU-based

[8] Of course, an adjustment of such a tolerance needs to be made before running the numerical experiments. For the cases reported herein, such oscillations occurred as the relative deviation reached levels around $(1 \sim 5)\times10^{-9}$. Additionally, it should be remembered that such computations also included the special enrichment functions.

solutions, among which the smoothest case has the worst error levels. Finally, the asymptotic convergence appears to have already been achieved when $b = 2$, whose convergence rates are close around the theoretical value.

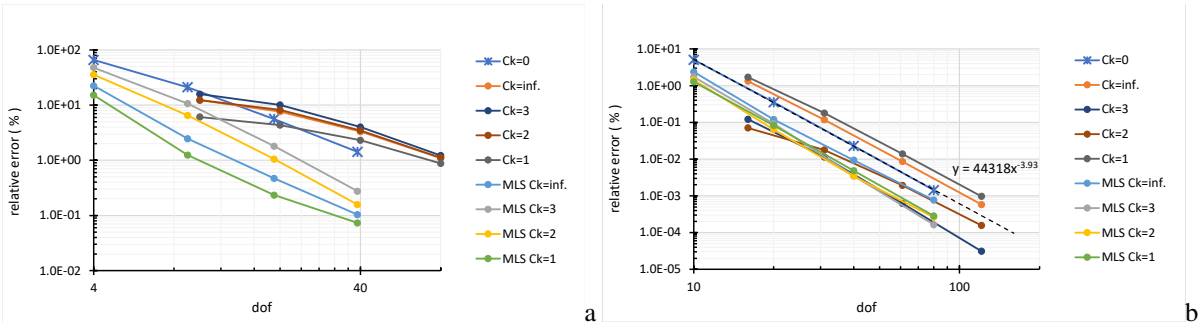

Figure 3. h-convergence for the polynomial solution. (a) Uniform degree $b = 1$. (b) Uniform degree $b = 2$.

4.2 Smooth (even analytic) solution with sign-changing second derivative in some small subdomain

For brevity, only the results for the mesh M20 are shown in the present text[9]. Figures 4 and 5 show the effects associated with the special enriched zone size, in case of basis with polynomial degree $b = 1$ and 2, respectively. In such figures, moving towards increasing abscissa values means larger zones with special enrichment.

In both situations, the error levels for the C^0-GFEM are higher than all the other approximations. Notably, for $b = 1$, the errors for the C^0 solutions seem to reach saturation at a level ten times higher than the worst case with MLS-PoUs.

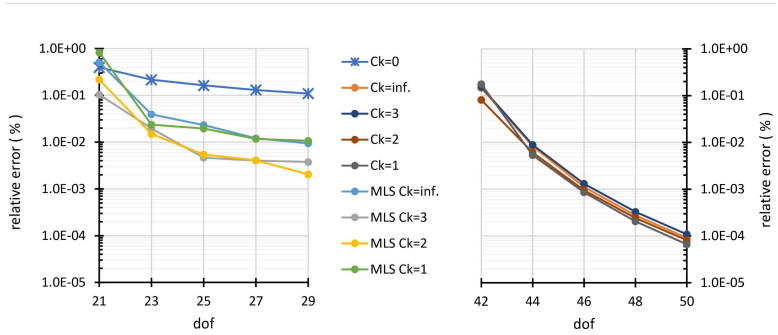

Figure 4. Error behavior once enlarging the enriched zone, problem with $b_2(x)$, mesh M20, with $b = 1$.

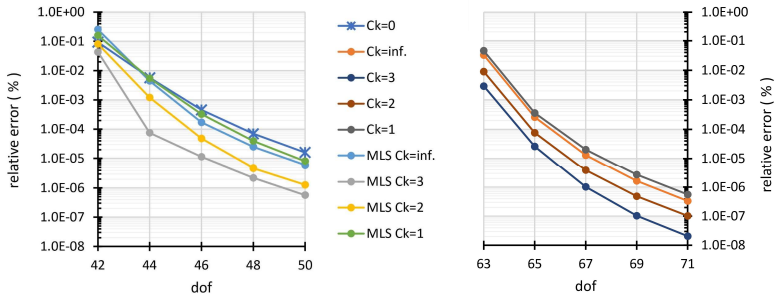

Figure 5. Error behavior once enlarging the enriched zone, problem with $b_2(x)$, mesh M20, with $b = 2$.

For $b = 1$, the C^k-GFEM solutions exhibit less tendency towards saturation, little sensitivity with relation to the smoothness, and a better ability to improve response as the enriched zone increases. When $b = 2$, all smooth solutions with smoothness orders $k = 2$ or 3 show smaller errors, indicating the inadequacy of the maximum continuity requirement.

[9] A more detailed explanation, considering the results for the remaining meshes, will be delivered at the presentation.

4.3 Solution with singular derivative at the left boundary

Once again, only the results for the mesh M20 are shown. Figures 6 and 7 show the effects associated with the special enriched zone size, in case of basis with polynomial degree $b = 1$ and 2, respectively.

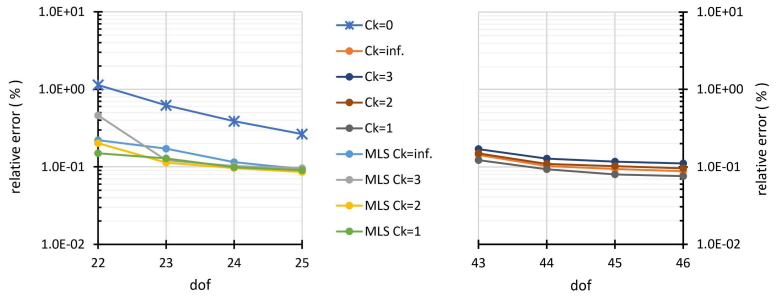

Figure 6. Error behavior once enlarging the enriched zone, problem with $b_3(x)$, mesh M20, with $b = 1$.

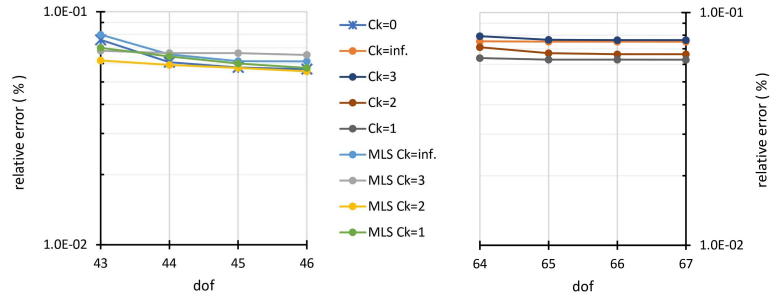

Figure 7. Error behavior once enlarging the enriched zone, problem with $b_3(x)$, mesh M20, with $b = 2$.

Notably, the PoU's continuity is very relevant when $b = 1$, because in both cases, with increased continuity, smaller errors occur even with smaller enriched zones. In the case of MLS-based PoUs, a smoothness order $k = 1$ performs better at the minimum enrichment. For the lower polynomial degree basis, the C^0-GFEM is susceptible to the size of the enriched zone. For this class of problem, the saturation occurs even for $b = 2$, for all approaches, and such saturation for C^k-GFEM occurs at a slightly higher level. The conventional GFEM, in the case of $b = 2$, performs as well as the best MLS-based approximation as the enriched zone increases.

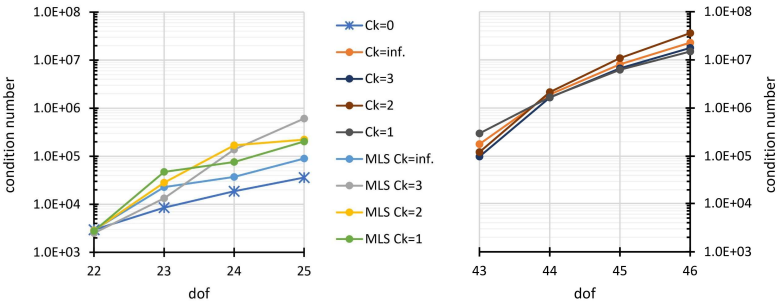

Figure 8. Condition number for the stiffness matrices, problem with $b_3(x)$, mesh M20, with $b = 1$.

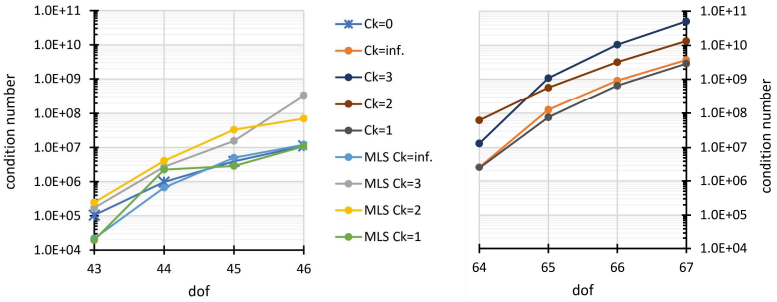

Figure 9. Condition number for the stiffness matrices, problem with $b_3(x)$, mesh M20, with $b = 2$.

Additionally, the stability if of very concern in the context of extrinsically enriched solutions. For this, figures 8 and 9 show the stiffness matrices condition number when applying enrichments with singular derivatives.

Notably, the condition number for the C^k-GFEM starts at a higher level and, for $b = 1$, there is practically no dependence on the smoothness order. However, the PoUs with enhanced consistency lead to conditioning comparable to that exhibit by the conventional GFEM. More surprisingly, in the case of $b = 2$, there are smoothness orders that virtually lead to the same conditioning of the C^0-GFEM, or even smaller, as occurs for the minimum enriched zone. It should be noted that such situations involve both special and polynomial enrichments.

5 Conclusions

A certain order of smoothness may be useful, actually, when applying enrichment functions to represent stress concentrations. It may deliver less sensitivity regarding to the size of the enriched zone. The most appropriate k parameter seems to depend on the specific characteristics of the enrichment function. When the smooth PoU already has the consistency of first degree, it is possible to benefit from the smoothness while requiring the same computational cost, in terms of dof, as the conventional C^0-GFEM, and yet not causing an impact on conditioning so intense as the C^k-GFEM in its original version.

Authorship statement. The author hereby confirm that he is the sole liable person responsible for the authorship of this work, and that all material that has been herein included as part of the present paper is either the property (and authorship) of the author, or has the permission of the owners to be included here.

References

[1] C. A. Duarte, D. J. Kim, and D. M. Quaresma. Arbitrarily smooth generalized finite element method. *Computer Methods in Applied Mechanics and Engineering*, vol. 196, n. 1-3, pp. 33–56, 2006.

[2] D. A. F. Torres, C. S. de Barcellos, and P. T. R. Mendonça. Smooth Generalized/eXtended FEM approximations in the computation of configurational forces in linear elastic fracture mechanics. *International Journal of Fracture*, vol. 219, n. 2, pp. 185–210, 2019.

[3] D. A. F. Torres. On the topological enrichment for crack modeling via the Generalized/eXtended FEM: a novel discussion considering smooth partitions of unity. *Engineering Computations*, vol. 38, n. 9, pp. 3517–3547, 2021.

[4] C. S. de Barcellos, P. T. R. Mendonça, and C. A. Duarte. A C^k continuous generalized finite element formulation applied to laminated Kirchhoff plate model. *Computational Mechanics*, vol. 44, pp. 377–393, 2009.

[5] P. T. T. Mendonça, C. S. de Barcellos, and D. A. F. Torres. Analysis of anisotropic Mindlin plate model by continuous and non-continuous GFEM. *Finite Elements in Analysis and Design*, vol. 47, n. 7, pp. 698–717, 2011.

[6] P. T. T. Mendonça, C. S. de Barcellos, and D. A. F. Torres. Robust C^k/C^0 generalized FEM approximations for higher-order conformity requirements: application to Reddy's HSDT model for anisotropic laminated plates. *Composite Structures*, vol. 96, pp. 332–345, 2013.

[7] D. A. F. Torres, C. S. de Barcellos, and P. T. R. Mendonça. Effects of the smoothness of partitions of unity on the quality of representation of singular enrichments for GFEM/XFEM stress approximations around brittle cracks. *Computer Methods in Applied Mechanics and Engineering*, vol. 283, pp. 243–279, 2015.

[8] M. Malagù, E. Benvenuti, C. A. Duarte, and A. Simone. One-dimensional nonlocal and gradient elasticity: assessment of high order approximation schemes. *Computer Methods in Applied Mechanics and Engineering*, vol. 275, pp. 138–158, 2014.

[9] M. Garbuio and D. A. F. Torres. Improving the polynomial reproducibility for the partition of unity in the C^k-generalized FEM. In E. P. Bandarra Filho, ed, *Proceedings of the twenty-fifth International Congress of Mechanical Engineering (XXV COBEM)*, Uberlândia. Brazilian Association of Engineering and Mechanical Sciences – ABCM, 2019.

[10] I. Babuška, J. R. Whiteman, and T. Strouboulis. *Finite elements: an introduction to the method and error estimation*. Oxford, New York, 2011.

[11] W. Rachowicz, J. T. Oden, and L. Demkowicz. Toward a universal h-p adaptive finite element strategy. part 3: Design of h-p meshes. *Computer Methods in Applied Mechanics and Engineering*, vol. 77, pp. 181–212, 1989.

[12] B. Szabó, A. Düster, and E. Rank. The p-version of the finite element method. In E. Stain, R. de Borst, and T. J. R. Hughes, eds, *Encyclopedia of Computational Mechanics*, volume 1, chapter 5, pp. 119–139. 1st edition, 2004.

[13] C. A. Duarte, I. Babuška, and J. T. Oden. Generalized finite element methods for three-dimensional structural mechanics problems. *Computers and Structures*, vol. 77, n. 2, pp. 215–232, 2000.